

Exciton polarizability in semiconductor nanocrystals

FENG WANG¹, JIE SHAN², MOHAMMAD A. ISLAM³, IRVING P. HERMAN³, MISCHA BONN⁴ AND TONY F. HEINZ^{1*}

¹ Departments of Physics and Electrical Engineering, Columbia University, New York, New York 10027, USA

² Department of Physics, Case Western Reserve University, Cleveland, Ohio 44106, USA

³ Department of Applied Physics and Applied Mathematics, Columbia University, New York, New York 10027, USA

⁴ FOM-Institute AMOLF, Kruislaan 407, 1098 SJ, Amsterdam, The Netherlands

*e-mail: tony.heinz@columbia.edu

Published online: 8 October 2006; doi:10.1038/nmat1739

The response of charge to externally applied electric fields is an important basic property of any material system, as well as one critical for many applications. Here, we examine the behaviour and dynamics of charges fully confined on the nanometre length scale. This is accomplished using CdSe nanocrystals^{1–3} of controlled radius (1–2.5 nm) as prototype quantum systems. Individual electron–hole pairs are created at room temperature within these structures by photoexcitation and are probed by terahertz (THz) electromagnetic pulses⁴. The electronic response is found to be instantaneous even for THz frequencies, in contrast to the behaviour reported in related measurements for larger nanocrystals⁵ and nanocrystal assemblies^{6,7}. The measured polarizability of an electron–hole pair (exciton) amounts to $\sim 10^4 \text{ \AA}^3$ and scales approximately as the fourth power of the nanocrystal radius. This size dependence and the instantaneous response reflect the presence of well-separated electronic energy levels induced in the system by strong quantum-confinement effects.

Isolated CdSe nanoparticles, also known as quantum dots (QDs), were prepared in our laboratory following established wet-chemistry procedures^{2,8}. The particle radius varied from 1.4 to 2.4 nm, with a standard deviation <5%. Because of the strong quantum confinement in these small QDs, the excited electron and hole are largely uncorrelated and can be described in a single-particle picture⁹. This system thus provides an attractive model for the study of the size dependence of the polarizability and response time of quantum-confined charge carriers. In addition to the fundamental interest inherent in these questions, an accurate determination of the behaviour of the quantum-confined electron–hole pairs provides important information about the excited states of the CdSe QDs, a topic of significant technological interest for the potential applications of QDs in lasers¹⁰, light-emitting diodes¹¹, photodetectors and other photovoltaic devices¹².

The polarizability of quantum-confined excitons has previously been examined using Stark shift measurements^{13–15}. It is desirable to have a direct experimental determination of the polarizability—

and its dependence on frequency and confinement size. Such measurements are, however, complicated by the fact that excitons must be produced by photoexcitation and then exist only for a duration of nanoseconds¹⁶. This situation suggests the use of a laser-based probe, an approach that can readily achieve the required temporal resolution and also has the advantage of being non-invasive in nature. In addition, such a probe must interrogate the system at sufficiently low photon energies to avoid complications from direct electron or hole transitions, which have energies of hundreds and tens of meV, respectively, for nanometre-sized QDs⁹. Terahertz (THz) time-domain spectroscopy meets these requirements: it allows the material response to an electric field oscillating at frequencies in the THz range (1 THz ≈ 4 meV) to be recorded with picosecond time resolution¹⁷. The capabilities of this technique for probing charge-carrier dynamics in photoexcited systems have been exploited in several recent studies. Among these are optical-pump/THz-probe measurements of charge transport and carrier dynamics in bulk solids^{18–24} and quantum-well structures^{25–27}. The method has also been applied, as mentioned above, to QDs extending to larger radii⁵ and to QD assemblies^{6,7}, as well as to carrier-cooling dynamics in QDs²⁸.

The experimental setup for the optical-pump/THz-probe apparatus has been described previously²⁹. Excitons in the semiconductor QDs were created by absorption of the frequency-doubled laser radiation with a photon energy of 3.1 eV. This energy lies well above the band edge of the QDs, which was located between 2.2 and 2.7 eV, depending on the QD radius. Care was taken to ensure that the induced material response remained in the linear regime as a function of pump fluence, with most photoexcited QDs containing only a single exciton. For this purpose and to avoid other nonlinear effects such as exciton photoionization, a pump fluence well below 1 J m^{-2} was used. All measurements were carried out with the sample held at room temperature.

To study the response of the CdSe QDs, we first measured the electric-field waveform $E(t)$ of the THz probe pulse transmitted through the unexcited sample. Subsequently, the pump-induced

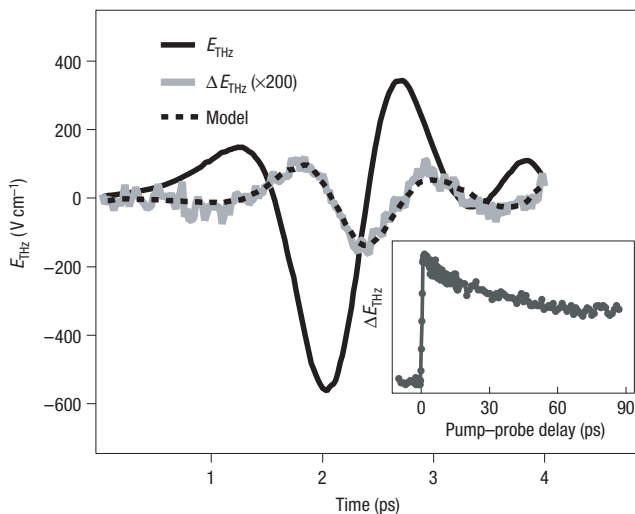


Figure 1 THz electric-field waveform transmitted through an unexcited suspension of CdSe QDs and the photoinduced change in this waveform. The dashed black line is the result of a calculation assuming a frequency-independent change in only the real part of the susceptibility. The inset depicts the decay of the pump-induced change in the transmission of the THz radiation. The photoinduced THz response was measured at 60 ps after photoexcitation.

change in the THz waveform $\Delta E(t)$ was recorded by chopping the excitation pulse and monitoring the differential THz signal (that is, with and without excitation). $\Delta E(t)$ was measured at a delay of 60 ps after the optical excitation. As shown in refs 16,30, exciton cooling in CdSe QDs occurs in ~ 1 ps. Thus, our measurement scheme ensures that we probe the ground-state exciton, despite initial optical pumping to higher-lying states. A modest reduction in the THz signal was observed with increasing pump/probe delays (inset of Fig. 1), which we attribute to carrier trapping at the QD interface in a subset of the QDs³¹. In our experiment, with a weak photoinduced change in a relatively thick sample, the effect of the pump beam can be expressed as a change in the complex sheet susceptibility of the sample, $\Delta \chi_s$, defined as the change in the dipole moment per unit area divided by the THz electric-field strength. Expressing the relevant quantities in the frequency domain²⁹, we have

$$\frac{\Delta E(\omega)}{E(\omega)} = i \frac{2\pi\omega}{c} \frac{\Delta \chi_s(\omega)}{\sqrt{\epsilon}}, \quad (1)$$

where c is the speed of light in vacuum, ω is the angular frequency of the THz radiation and ϵ is the dielectric function of the unexcited QD suspension.

In Fig. 1 we show experimental results for the transmitted THz field $E(t)$ and the photoinduced modulation $\Delta E(t)$ for CdSe QDs of 2.0 nm radius. Figure 2 shows the corresponding frequency-dependent changes in the sheet susceptibility $\Delta \chi_s(\omega) = \Delta \chi'_s(\omega) + i \Delta \chi''_s(\omega)$, as calculated from the experimental data and equation (1). The imaginary part of the susceptibility is seen to remain essentially unchanged, whereas the change in the real part is appreciable, but largely frequency-independent over the investigated frequency range. Indeed, the experimental waveform for the response, $\Delta E(t)$, can be reproduced numerically by propagating the measured $E(t)$ through a sample with a frequency-independent real susceptibility $\Delta \chi_s(\omega) = \Delta \chi'_s$ (dashed lines in Figs 1 and 2). This response is entirely different from that observed in a test measurement of a photoexcited CdSe thin film (data not shown). For the latter case, we found a Drude-like THz response

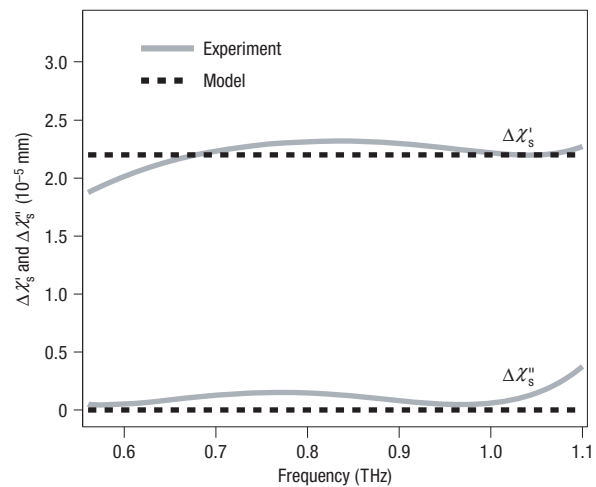


Figure 2 Spectral dependence of the change in the real ($\Delta \chi'_s$) and imaginary part ($\Delta \chi''_s$) of the photoinduced sheet susceptibility of the sample. The grey lines are obtained from the experimental data of Fig. 1. The dashed lines represent a frequency-independent and purely real induced susceptibility that corresponds to the dashed waveform in the time-domain data of Fig. 1.

characteristic of free charges and similar to the behaviour in other doped or photoexcited semiconductors⁴.

Classical transport theory—adapted from the bulk material with an added term accounting for surface scattering—has been used to model the THz response of nanoparticles with radii up to 12.5 nm (ref. 5). Such a description is not, however, appropriate for the small QDs under investigation here. In these QDs, strong confinement effects occur and the carriers occupy discrete energy levels separated by at least tens of meV (ref. 9). This situation invalidates the picture of perturbed bulk transport with charge carriers moving in a continuous band of states. In the strong confinement regime, the excitations are more like those of a large atom than those of a small piece of bulk material. We consequently consider our measurement as probing the polarizability of the photogenerated exciton confined in QDs. From the experimental standpoint, the correctness of this view is confirmed by the observation that the response to a THz electric field (Fig. 2) is given by a real and spectrally flat susceptibility. These two features both follow from the existence of well-separated electronic states that are probed by THz radiation with photon energies (of ~ 4 meV) lying significantly below the electron and hole transitions.

The experimental measurements yield information about the THz response of the quantum-confined excitons through the sheet susceptibility of the photoexcited sample. We can relate this quantity to the exciton polarizability α of an individual excited QD by

$$\Delta \chi_s = n_s \frac{9\epsilon^2}{(\epsilon_{NP} + 2\epsilon)^2} \alpha. \quad (2)$$

Here $\epsilon = 1.81$ is the measured dielectric constant of the suspension, $\epsilon_{NP} \approx 10$ is the dielectric constant of the unexcited CdSe (ref. 32) and n_s is the sheet excitation density. The last quantity is given by the number of incident photons per unit area for our optically dense sample, which is assumed to have unity quantum efficiency for exciton generation⁸. The relation given in equation (2) follows from the effective-medium theory³³ in the (experimentally relevant) dilute limit, but without any self-screening of the exciton.

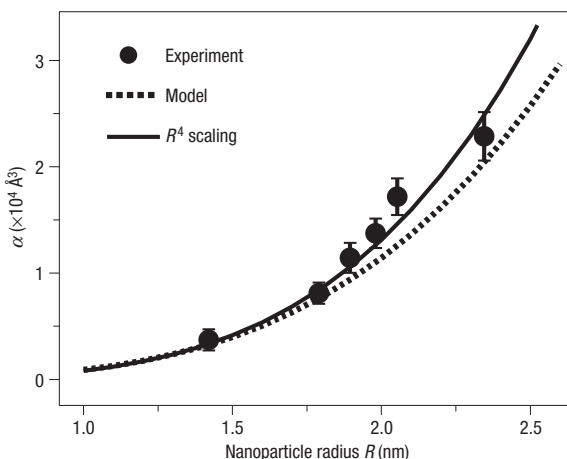


Figure 3 Polarizability of quantum-confined excitons in photoexcited CdSe QDs as a function of the QD radius R . Experimental data (symbols) and theoretical predictions based on the multiband effective-mass model described in the text (dotted line). For comparison, the solid line shows a simple R^4 scaling. The error bars reflect the reproducibility of the measurements; in addition, there is an overall uncertainty of a factor of 2 in the vertical scale associated with the experimental determination of the QD excitation density.

The exciton polarizability α derived in this manner is shown in Fig. 3 as a function of the size of the QD. The numerical values of the polarizability are of the order of $10,000 \text{ Å}^3$, three orders of magnitude larger than typical molecular polarizabilities and about 10 times larger than that of conjugated oligomer chains of similar length³⁴. These results are qualitatively consistent with those of d.c. Stark effect measurements, which also indicate very large polarizabilities^{13–15}. The error bars for α in Fig. 3 correspond to the reproducibility of the measurement. Because of inhomogeneities in the spatial profile of the pump beam and possible residual effects of multiple electron–hole pair excitation in the QDs, the overall vertical scale is subject to an estimated error up to a factor of 2.

The measured dependence of the polarizability on the QD radius R can be described reasonably well by the scaling relation $\alpha \sim R^4$ (solid line in Fig. 3). This behaviour can be understood from the usual expression for the linear polarizability: $\alpha \sim |e\mathbf{r}|^2/\Delta E$, where $e\mathbf{r}$ is the transition dipole moment and ΔE is a typical energy-level spacing of the charge carrier. For a carrier confined within a region of characteristic size R , the dipole moment is of the order of eR and the energy-level spacing is $\sim h^2/mR^2$, where m is the mass of the charge carrier and h is Planck's constant. Thus, $\alpha \sim R^4/a_B$ is obtained, where a_B denotes the Bohr radius.

To describe the exciton polarizability more quantitatively, including both its magnitude and variation with R , we use a more realistic model of the electronic structure of the QDs within a multiband effective-mass treatment⁹. In the regime of interest with $R < a_B$ ($\sim 5 \text{ nm}$ for CdSe), it has been shown that both the energy levels and wavefunctions for the electron and hole comprising an exciton are largely uncorrelated⁹. Consequently, we can analyse the excitations within a single-particle picture⁹ and treat the exciton polarizability as the sum of contributions from the electron and the hole, with correction from the interactions treated perturbatively. In this picture, we obtain the relevant energies and transition strengths for the electron and hole separately and evaluate their contributions to the polarizability (see the Supplementary Information). The calculations reveal that the hole contribution to the polarizability dominates over that from the electron, owing to

a larger hole effective mass and the concomitant smaller energy-level spacing. Figure 3 (dotted line) shows the resulting predictions for the polarizability as a function of QD radius R . The analysis yields a size dependence of $\alpha \sim R^{3.6}$ for the polarizability over the relevant range of QD radii. The modest deviation from the simple R^4 scaling arises from the non-parabolicity of the electronic bands and from the electron–hole interaction. The latter effect would cause α to level off as the size of the QD increases and bulk excitonic effects emerge. The agreement with the experimentally derived polarizabilities is surprisingly good considering the experimental uncertainties and the simplifications inherent in the model.

In the strongly confined QDs studied here, the exciton response is ‘atom’-like, characterized by a large polarizability with an instantaneous response up to THz frequencies. A systematic investigation of QDs of increasing radius will permit the understanding of possible pathways of the cross-over from this strongly confined ‘atomic’ response to different types of bulk behaviour involving excitons or free carriers.

METHODS

SAMPLE PREPARATION

QDs, capped by TOPO (trioctylphosphine oxide, Aldrich), TOP (trioctylphosphine, Aldrich), and ~ 1.5 monolayer of ZnS were synthesized in our laboratory by wet chemistry^{2,8}. The radii of the QDs and their size distribution in any given sample were deduced from the position and width of the first peak of the absorption spectra following ref. 3. The QDs were probed in a 1 cm cell containing a dilute suspension of the particles (concentration $< 10^{16} \text{ cm}^{-3}$) in 2,2,4,4,6,6,8-heptamethylnonane (Aldrich).

EXPERIMENTAL SETUP

The femtosecond laser source consisted of an amplified, mode-locked Ti:sapphire system, providing pulses of approximately 200 fs duration at 810 nm with an energy of 1 mJ per pulse and a repetition rate of 1 kHz. The THz system³⁵ used optical rectification of the femtosecond laser pulses in a ZnTe crystal for the generation of the THz probe field. The detection of the THz waveform was accomplished by electro-optic sampling with a time-synchronized femtosecond laser pulse in a second ZnTe crystal.

Received 9 April 2006; accepted 21 August 2006; published 8 October 2006.

References

- Woggon, U. *Optical Properties of Semiconductor Quantum Dots* (Springer, Berlin, 1997).
- Murray, C. B., Norris, D. J. & Bawendi, M. G. Synthesis and characterization of nearly monodisperse CdE (E = S, Se, Te) semiconductor nanocrystallites. *J. Am. Chem. Soc.* **115**, 8706–8715 (1993).
- Norris, D. J. & Bawendi, M. G. Measurement and assignment of the size-dependent optical spectrum in CdSe quantum dots. *Phys. Rev. B* **53**, 16338–16346 (1996).
- Schmuttenmaer, C. A. Exploring dynamics in the far-infrared with terahertz spectroscopy. *Chem. Rev.* **104**, 1759–1779 (2004).
- Beard, M. C., Turner, G. M. & Schmuttenmaer, C. A. Size-dependent photoconductivity in CdSe nanoparticles as measured by time-resolved terahertz spectroscopy. *Nano Lett.* **2**, 983–987 (2002).
- Beard, M. C. *et al.* Electronic coupling in InP nanoparticle arrays. *Nano Lett.* **3**, 1695–1699 (2003).
- Cooke, D. G. *et al.* Anisotropic photoconductivity of InGaAs quantum dot chains measured by terahertz pulse spectroscopy. *Appl. Phys. Lett.* **85**, 3839–3841 (2004).
- Hines, M. A. & Guyot-Sionnest, P. Synthesis and characterization of strongly luminescing ZnS-capped CdSe nanocrystals. *J. Phys. Chem.* **100**, 468–471 (1996).
- Efros, A. L. & Rosen, M. The electronic structure of semiconductor nanocrystals. *Annu. Rev. Mater. Sci.* **30**, 475–521 (2000).
- Klimov, V. I. *et al.* Optical gain and stimulated emission in nanocrystal quantum dots. *Science* **290**, 314–317 (2000).
- Colvin, V. L., Schlamp, M. C. & Alivisatos, A. P. Light-emitting diodes made from cadmium selenide nanocrystals and a semiconducting polymer. *Nature* **370**, 354–357 (1994).
- Ginger, D. S. & Greenham, N. C. Charge injection and transport in films of CdSe nanocrystals. *J. Appl. Phys.* **87**, 1361–1368 (2000).
- Empedocles, S. A. & Bawendi, M. G. Quantum-confined Stark effect in single CdSe nanocrystallite quantum dots. *Science* **278**, 2114–2117 (1997).
- Sacra, A., Norris, D. J., Murray, C. B. & Bawendi, M. G. Stark spectroscopy of CdSe nanocrystallites—the significance of transition linewidths. *J. Chem. Phys.* **103**, 5236–5245 (1995).
- Seufert, J. *et al.* Stark effect and polarizability in a single CdSe/ZnSe quantum dot. *Appl. Phys. Lett.* **79**, 1033–1035 (2001).
- Klimov, V. I. Optical nonlinearities and ultrafast carrier dynamics in semiconductor nanocrystals. *J. Phys. Chem. B* **104**, 6112–6123 (2000).

17. Beard, M. C., Turner, G. M. & Schmuttenmaer, C. A. Terahertz spectroscopy. *J. Phys. Chem. B* **106**, 7146–7159 (2002).
18. Groeneweld, R. H. M. & Grischkowsky, D. Picosecond time-resolved far-infrared experiments on carriers and excitons in GaAs-AlGaAs multiple-quantum wells. *J. Opt. Soc. Am. B* **11**, 2502–2507 (1994).
19. Hegmann, F. A., Tykwinski, R. R., Lui, K. P. H., Bullock, J. E. & Anthony, J. E. Picosecond transient photoconductivity in functionalized pentacene molecular crystals probed by terahertz pulse spectroscopy. *Phys. Rev. Lett.* **89**, 227403 (2002).
20. Thorsmolle, V. K. *et al.* Ultrafast conductivity dynamics in pentacene probed using terahertz spectroscopy. *Appl. Phys. Lett.* **84**, 891–893 (2004).
21. Huber, R. *et al.* How many-particle interactions develop after ultrafast excitation of an electron–hole plasma. *Nature* **414**, 286–289 (2001).
22. Shan, J., Wang, F., Knoesel, E., Bonn, M. & Heinz, T. F. Measurement of the frequency-dependent conductivity in sapphire. *Phys. Rev. Lett.* **90**, 247401 (2003).
23. Averitt, R. D. *et al.* Ultrafast conductivity dynamics in colossal magnetoresistance manganites. *Phys. Rev. Lett.* **87**, 17401 (2001).
24. Beard, M. C., Turner, G. M. & Schmuttenmaer, C. A. Transient photoconductivity in GaAs as measured by time-resolved terahertz spectroscopy. *Phys. Rev. B* **62**, 15764–15777 (2000).
25. Turchinovich, D. *et al.* Ultrafast polarization dynamics in biased quantum wells under strong femtosecond optical excitation. *Phys. Rev. B* **68**, 241307 (2003).
26. Muller, T., Parz, W., Strasser, G. & Unterrainer, K. Pulse-induced quantum interference of intersubband transitions in coupled quantum wells. *Appl. Phys. Lett.* **84**, 64–66 (2004).
27. Kaindl, R. A., Carnahan, M. A., Hagele, D., Lovenich, R. & Chemla, D. S. Ultrafast terahertz probes of transient conducting and insulating phases in an electron–hole gas. *Nature* **423**, 734–738 (2003).
28. Hendry, E. *et al.* Direct observation of electron-to-hole energy transfer in CdSe quantum dots. *Phys. Rev. Lett.* **96**, 057408 (2006).
29. Knoesel, E., Bonn, M., Shan, J. & Heinz, T. F. Charge transport and carrier dynamics in liquids probed by THz time-domain spectroscopy. *Phys. Rev. Lett.* **86**, 340–343 (2001).
30. Underwood, D. F., Kippeny, T. & Rosenthal, S. J. Ultrafast carrier dynamics in CdSe nanocrystals determined by femtosecond fluorescence upconversion spectroscopy. *J. Phys. Chem. B* **105**, 436–443 (2001).
31. Guyot-Sionnest, P., Shim, M., Matranga, C. & Hines, M. Intraband relaxation in CdSe quantum dots. *Phys. Rev. B* **60**, R2181–R2184 (1999).
32. Lide, D. R. *Handbook of Chemistry and Physics* (CRC Press, New York, 1999).
33. Choy, T. C. *Effective Medium Theory—Principles and Applications* (Oxford Science Publications, Oxford, 1999).
34. Gelinck, G. H. *et al.* Measuring the size of excitons on isolated phenylene-vinylene chains: From dimers to polymers. *Phys. Rev. B* **62**, 1489–1491 (2000).
35. Nahata, A., Weling, A. S. & Heinz, T. F. A wideband coherent terahertz spectroscopy system using optical rectification and electro-optic sampling. *Appl. Phys. Lett.* **69**, 2321–2323 (1996).

Acknowledgements

Research at Columbia University was supported primarily by the MRSEC Program of the National Science Foundation under award number DMR-0213574 and by the New York State Office of Science, Technology and Academic Research (NYSTAR), with additional support from US Department of Energy, Office of Basic Energy Sciences, through the Catalysis Science Program. Work at Case Western Reserve University was supported by NSF grant DMR-0349201. Correspondence and requests for materials should be addressed to T.F.H. Supplementary Information accompanies this paper on www.nature.com/naturematerials.

Competing financial interests

The authors declare that they have no competing financial interests.

Reprints and permission information is available online at <http://npg.nature.com/reprintsandpermissions/>